Self-Adaption AAE-GAN for Aluminum Electrolytic Cell Anomaly Detection

DANYANG CAO [1,2], **DI LIU** [1], **XU REN** [1], **AND NAN MA** [3], **(Senior Member, IEEE)**

[1]School of Information Science and Technology, North China University of Technology, Beijing 100144, China
[2]Beijing Key Laboratory on Integration and Analysis of Large-Scale Stream Data, Beijing 100144, China
[3]College of Robotics, Beijing Union University, Beijing 100101, China

Corresponding author: Danyang Cao (ufocdy@163.com)

ABSTRACT Nowadays, the anomaly detection of aluminum electrolysis cell is a big problem in the aluminum electrolysis industry. The problem of unbalanced time series samples is common in industrial applications. The number of samples under normal conditions is much larger than that under abnormal conditions. In the electrolytic aluminum industry, this problem is even more serious, it is very difficult to find abnormal samples in industrial production because experts do not have a clear criterion to judge abnormalities. In traditional machine learning algorithms, such as support vector machine (SVM) and convolutional neural network (CNN), it is difficult to obtain high classification accuracy on the problem of class imbalance, and these methods tend to be more biased towards positive samples. In recent years, generative adversarial network (GAN) has become more and more popular in the field of anomaly detection. However, these methods need to find the best mapping from the actual space to the latent space in the anomaly detection stage, and the optimization process may bring new errors and take a long time. In this article, we use the ability of GAN to model complex high-dimensional image distribution, and propose a self-adaption AAE-GAN network based on adaptive changes of input samples. This time series anomaly detection method converts multi-dimensional time series data into a two-dimensional matrix, and only normal samples are needed in the training process, which effectively solves the above problems. The method we proposed is to use encoder and decoder to constitute a generator and a discriminator. During the training process, the generator and the discriminator are trained jointly and confrontationally, so that the mapping ability of the encoder can be fully reflected. In the anomaly detection stage, we determine whether the sample is abnormal according to the size of the reconstruction difference. Experimental results show that the detection accuracy and speed of this method are very high.

INDEX TERMS Aluminum electrolytic cell, anomaly detection, AAE-GAN, multivariate time series, imbalanced industrial time series.

I. INTRODUCTION

In recent years, due to the increasing development of the Industrial Internet, industrial big data has become a very popular research topic. In industrial production, due to the complexity of production, the large number of sensors used and the high sampling frequency, industrial equipment can easily accumulate a large amount of time series data in a short period of time [1], [2]. Certain abnormal situations that occur during the production process will cause damage to industrial equipment. An abnormality in the working process of the aluminum electrolytic cell may cause damage to the

electrolytic cell and waste of production materials, which will greatly increase the cost of production. Through the implementation of early preventive maintenance, early detection of abnormalities can improve the equipment production efficiency. The characteristics of industrial time series data include large scale and long period. To help domain experts make key decisions quickly and design an effective anomaly detection method is a very valuable work, which is also the work of this article.

When an observation is very different from other observations, so that we suspect that they are produced by different mechanisms, such points become abnormal, also called outliers [3], [4]. The concept of time series anomaly is also put forward by most scholars based on this definition

The associate editor coordinating the review of this manuscript and approving it for publication was Sunil Karamchandani.

and related practical applications. Nowadays, the research of anomaly detection is involved in various data fields, including high-dimensional data, uncertain streaming data, network data and time series data [5]–[12]. A lot of work has been spent on the research of time series anomaly detection. Through our literature review, we found several time series anomaly detection models, including autoregressive integral moving average (ARIMA), cumulative sum statistics (CUSUM), exponentially weighted moving average (EWMA), Bayesian classifier, support vector machine (SVM), neural networks, deep learning methods, etc. [13]–[21]. However, due to the large scale and long period of industrial time series data, traditional time series anomaly detection methods cannot meet people's actual needs. Moreover, because of the fact that the industrial data violates the assumption of sample balance: positive samples are much larger than abnormal samples, the above methods cannot achieve high accuracy in industrial data sets [22]. In the past research, many anomaly detection studies often used unsupervised methods based on deep learning [23], [24]. Many scholars use the difference between the predicted value and the actual value at each time point to detect anomalies. On this basis, neural networks are used to learn the unknown relationships in time series data and establish prediction models [25], [27]. For example, Hundman *et al.* established a long short-term memory (LSTM) prediction model based on normal time series data, which identified anomalies by comparing the difference between the predicted value and the true value at each time point [26]. Malhotra *et al.* conducted a study on judging anomalies in time series data at multiple time steps, and proposed a stacked LSTM network trained on normal data [28]. Other predictive models include multi-layer perceptron (MLP) and support vector regression (SVR). With the development of industrial systems, time series data has become more and more complex. In the process of industrial production, due to different usage methods and unpredictable external factors, the behavior produced by the machine is always changing [29]. In this case, it is difficult to predict the future time series even if the data in several time steps are integrated, which leads to a greatly reduced accuracy of the time series anomaly detection method based on the prediction model.

In order to solve the above problems, some models based on sample reconstruction have been proposed by scholars. This method uses an autoencoder (AE) to detect abnormalities. The job of the encoder is to learn the latent representation of the input time series, and the job of the decoder is to use the generated latent representation to reconstruct the original time series, and determine whether the sample is abnormal by reconstructing the size of the difference [30]–[33]. Among many methods based on sample reconstruction, AE is a representative model, which is a network that combines encoder and decoder. After this method was proposed, technologies such as sliding window and variational autoencoder (VAE) were also applied to this idea for anomaly detection of time series data.

In [34], a time series anomaly detection method based on sliding window and sample reconstruction was proposed. Subsequently, in [29], some time series anomaly detection methods based on VAE were proposed. The difference between model VAE and model AE is that VAE models the potential probability distribution of the sample through variational inference. Not long ago, Goodfellow *et al.* proposed a generative adversarial network (GAN) [35], which provided a new solution for industrial time series anomaly detection. The original purpose of the model is to use for image recognition and sample generation. The basic idea of GAN is to use a generator to generate samples that people need from random data points that meet a specific distribution (for example, Gaussian distribution). Some scholars use the ability of GAN to learn images and apply it to the field of image anomaly detection, such as AnoGAN [36], BiGAN [37] and GANomaly [38] and some GAN-based imbalanced data intrusion detection models [61]–[63]. These GAN-based network architectures have shown high performance. These methods only need normal samples in the training phase, and perform anomaly detection through the difference between normal samples and abnormal samples in the test phase. From this point of view, these GAN-based methods are very effective for sample imbalance problems and can prevent the model judgment result is biased towards the normal sample. However, in industrial applications, GAN-based anomaly detection methods are rarely seen, and the expected results cannot be achieved. [39], [40] proposed a GAN-based mechanical anomaly detection model. [41] proposed a GAN-based anomaly diagnosis method for sample imbalance. [42] proposed a GAN-based model to detect cyber-attacks from cyber-physical system. Recently, scholars have proposed a relatively novel GAN-based industrial time series anomaly detection method [43]. Since the LSTM network is more popular in the field of time series, this method adds the LSTM network to the generator and the discriminator respectively, and its purpose is to better learn the distribution of time series. However, this method has a flaw. It needs to find the best mapping from the actual distribution to the potential distribution in the anomaly detection stage. In the process of finding the best mapping, new errors are likely to occur, and it will also increase the time of anomaly detection. The system cannot report errors in a timely manner. In summary, GAN has been successfully applied in the field of image anomaly detection, which proves the ability of GAN to learn complex high-dimensional image distribution. The above researches have inspired us to use GAN's ability to learn images to solve industrial anomaly detection problems, especially for no abnormalities.

The earth's crust contains a lot of aluminum, which is second only to oxygen and silicon, ranking third, and is the metal element with the highest content in the earth's crust. However, due to the very active chemical properties of metallic aluminum, aluminum in the state of pure metallic elements rarely exists in nature. As we all know, aluminum has good electrical conductivity and corrosion resistance, and can easily form

aluminum alloy with other metal elements. Therefore, it is widely used in transportation, electric power, construction, mechanical packaging and aerospace industries. It is called ''universal metal''. In the initial stage, people used chemical reduction methods to produce metal aluminum, such as the use of sodium potassium compounds for reduction and extraction. Until 1886, Hall and Erou, from the United States and France, invented the aluminum oxide molten salt electrolysis method. Since then, the method of using electrolytic technology to manufacture metallic aluminum has been continued to this day.

The actual production process of electrolytic aluminum is mainly completed inside the electrolytic cell, in which the alumina melt is the main electrolyte, and the two poles are mainly composed of carbon materials. After the electrolytic cell is energized, the current is introduced from the anode of the electrolytic cell, inside the body and passes through the electrolyte layer, flows to the cathode of the electrolytic cell and finally flows out of the electrolytic cell. Under the action of this direct current, the originally crystalline alumina can be melted. In addition, the electrolyte undergoes an electrochemical reaction under the action of the electric current. The aluminum ions obtain electrons from the cathode of the electrolytic cell and are precipitated to obtain aluminum liquid. With the continuous operation of the electrolytic cell, the content of liquid aluminum will continue to increase. After the aluminum liquid has accumulated to a certain extent, it can be sucked out of the electrolytic cell by a vacuum ladle and sent to the foundry workshop, and then undergoes a series of subsequent processing, finally casts to produce aluminum ingots.

In this paper, inspired by GANomaly [38], for unbalanced industrial data, we propose a self-adaption changing adversarial autoencoders generative adversarial network (self-adaption AAE-GAN) to solve the above problem. The model consists of a generator and a discriminator. The generator is composed of two sub-networks, an autoencoder group based on a deep convolution generation confrontation network and an encoder. In order to improve the accuracy of anomaly detection, we propose a method to adaptively change the model structure. According to the complexity of the input samples, we change the number of decoder-encoder and convolutional/deconvolutional layers in the autoencoder group. At the same time, in order to reduce the training time and improve the performance of the model, a feature extraction step is inserted between the original data and the GAN. Since the encoder, generator and discriminator are jointly trained in the training phase, there is no need to calculate the best mapping from real-time space to latent space in the anomaly detection phase. The time required for the anomaly detection phase is greatly reduced, which allows our model to detect anomalies faster. At the same time, due to the joint optimization of all components in our model, our model has a higher accuracy rate in anomaly detection. Our model is compared with the other three networks used to solve the class imbalance problem on three datasets.

The experimental results show that our method has an excellent anomaly detection performance.

The main contributions of this paper are as follows: 1) Aiming at the problem of unbalanced time series samples in the field of aluminum electrolysis, using the ability of GAN to learn the distribution of complex high-dimensional images, a new anomaly detection method based on GAN is proposed. 2) In order to increase the anomaly detection accuracy of the model, a self-adaption AAE-GAN time series anomaly detection method based on the adaptive change of input samples is proposed. 3) We propose a model that only requires normal samples in the training phase. 4) The anomaly score is composed of the weighted average of the two reconstruction differences in the generator part.

II. RELATED WORK

For a long time, anomaly detection has been a hot issue in industrial systems. Now scholars have published a large number of papers and put forward many effective theories and algorithms.

A. INTELLIGENT FAULT DIAGNOSIS MODEL BASED ON DEEP LEARNING

Nowadays, various industrial production processes are getting more and more refined, and the amount and complexity of the time series are increasing, which make the deep learning more and more popular in the field of industrial anomaly detection [44]. These methods use black box patterns to extract specific feature patterns for specific datasets. Since these methods are mostly based on unsupervised architectures, they do not know what the final output features are. Representative models include LSTM [45], recurrent neural network (RNN) [46], convolutional neural network (CNN) [47] and AE [48]. Although the above-mentioned deep learning models are very popular in the field of anomaly detection, their performance cannot meet people's expectations when faced with industrial datasets with unbalanced samples. In addition, due to the diversified forms of industrial data, training data may consist of images or time series data. Many deep learning models are only applicable to a single field, but it is usually difficult to apply them to industrial fields.

B. MODEL BASED ON CLASS IMBALANCE PROBLEM

In order to solve the problem of unbalanced time series anomaly detection, scholars have proposed two methods: one is based on the data direction, and the other is based on the algorithm direction [49]–[51] proposed two methods based on data direction, they used sampling strategies, such as under-sampling and over-sampling techniques to improve the problem of sample imbalance [52]. In [50], a method based on the direction of the algorithm was proposed, which solved the problem of sample imbalance by improving the performance of the classifier, and using techniques such as bagging and enhanced integration. In [49] and [53], scholars have proposed EasyEnsemble and BalanceCascade algorithms to

solve the problem of class imbalance. In addition to improving the classifier, a synthetic minority oversampling technique (SMOTE) algorithm was proposed in [54] and [55] to synthesize samples of a few categories to solve the problem of class imbalance. In some industrial production, there may be multiple types of unbalanced problems. In order to solve this problem, [49] has proposed an Easy-SMT integrated algorithm based on the SMOTE algorithm and the EasyEnsemble algorithm.

C. GAN-BASED MODEL

In recent years, GAN has become more and more popular in the field of image anomaly detection with imbalances. GAN is an unsupervised network architecture based on deep learning. It was originally proposed by Goodfellow to solve the problems of image recognition and image generation. After GAN was proposed, many variant models were proposed by scholars to use adversarial algorithms to solve various problems. For more detailed information, please refer to [56]. This article provides a lot of introductions to GAN.

In the field of anomaly detection, Lim *et al.* combined GAN with LSTM-RNN and proposed an anomaly detection method for detecting cyber-physical systems' network attacks. In order to improve the performance of the model, the author proposed a GAN-based data enhanced technology and achieved good results [57]. At the same time, Samet *et al.* [38] proposed a GANomaly image anomaly detection model. In this paper, the author compares the GANomaly model with the current popular image anomaly detection methods. This method uses benchmark datasets such as MNIST and CIFAR10 to verify the performance advantages of the model [38], which has prompted us to combine image anomaly detection technology with the aluminum electrolysis industry. The following is a brief introduction of GANomaly: The most attractive part of the model is the generator network. Samet *et al.* [38] use the encoder-decoder-encoder architecture to form the generator network of the GANomaly model, where the encoder, decoder and discriminator network use a deep convolutional generative confrontation network (DCGAN) [58]. In the training process, the model uses three loss functions to learn the mode of mutual conversion between the latent representation of the image and the actual feature, and uses the reconstruction difference of the image to perform anomaly detection. The characteristic of this model is that no abnormal samples are needed in the training process; this means that only normal samples are needed for model training, the problem of sample imbalance is solved well, and it shows high anomaly detection performance.

D. ANOMALY DETECTION MODEL IN ALUMINUM ELECTROLYTIC CELL

Li Tian *et al.* [64] proposed an improved LMD decomposition method, that was used to decompose the cell voltage signal based on wavelet packet denoising. At the same time, according to the energy analysis, the extracted features were classified. They analyzed the voltage signal and extracted features for abnormality detection. This approach is not precise enough, because the abnormality of the electrolytic cell is determined by multiple factors, and it is not possible to just observe the change of the voltage signal to draw a conclusion. Enji Sun *et al.* [65] proposed an aluminum cell condition diagnosis and decision system to detect heat radiation. Their method was also used to judge the abnormality of the electrolytic cell which was only based on the temperature, and the abnormal state of the electrolytic cell was divided into many types, which might not be reflected in the temperature. Chen Xiaofang *et al.* [66] considered the strong link between the fire hole observation and superheat degree, a method of superheat degree identification based on computer vision technology and expert rules was proposed. Their method is similar to the above methods, and the detection method is not comprehensive enough.

The rest of this article is organized as follows: Section 3 proposes our anomaly detection framework based on GAN. The experimental setup and results are described in the third part and the fourth part respectively. Finally, conclusions and future work are drawn in Section 5.

III. METHOD

Aiming at the problem of the imbalance of time series samples in the field of aluminum electrolysis, we use the ability of GAN to learn the distribution of complex high-dimensional images, and propose a new anomaly detection method based on GAN. In the following section, we will introduce the structure and training process of this model.

A. SELF-ADAPTION AAE-GAN

This paper proposes a self-adaption AAE-GAN, which is a time series anomaly detection method based on the adaptive change of input samples. This method has two stages, one is the model training stage and the other is the anomaly detection stage. In the training phase, our model only learns the distribution of normal time series data. In the testing phase, we judge whether the sample is an abnormal sample based on the abnormal score A(x) output by the model. The higher the anomaly score, the higher the probability that the sample is anomalous. Fig. 1 shows the architecture of GAN, including adversarial autoencoders which are based on adaptively changing of input samples.

Our model is divided into two parts. The entire network is composed of a generator and a discriminator, and the generator is composed of an encoder and multiple autoencoder groups.

The generator consists of an encoder and multiple autoencoder groups. A group of autoencoder consists of an encoder and a decoder, and form the generator of the model. Its structure is as follows:

$$G = E\left(\hat{x}\right) + m1 * (G_D\left(z\right) + G_E\left(x\right)) \tag{1}$$

In order to increase the accuracy of model anomaly detection and reduce the training time of the model, the number

TABLE 1. The influence of m1.

m1	1	2	3	4	5	6	7	8
Precision	0.790	0.830	0.851	0.860	0.856	0.861	0.862	0.859
Avg Run Time (ms/batch)	10.380	17.093	22.427	29.831	48.530	67.258	88.109	120.063

of autoencoder groups is determined by the dimension and density of the input samples. The higher the dimension and density of the two-dimensional matrix, the higher the number of autoencoder groups is. In the process of increasing the number of autoencoder groups, although the accuracy of the model has been improved, it will also be accompanied by an increase in model training time, so the number of autoencoder groups cannot be increased blindly. The number of m1 in (1) is determined by the following formula:

$$m1 = \frac{dim(x)}{16} * [0.5 + den(x)] + k1, \, k1$$
$$= 0, 1, 2, \ldots, n$$
$$den(x) = \frac{N_V}{N_S} \tag{2}$$

where dim(x) is the dimension of two-dimensional matrix, N_V is the number of data points with value, and N_S is the total data points. The maximum value of m1 cannot exceed the threshold $_3 = 7$. With the increase of m1, the average running time and accuracy are as follows:

After exceeding 7, the training time of the model will greatly increase, but the accuracy of the model does not increase significantly. So, we set the threshold to 7. The model consists of three sub-networks.

The first sub-network is the autoencoder group DE. G_E and G_D are a part of the autoencoder group DE. G_E is an encoder and G_D is a decoder. The generator learns the input image data and reconstructs the input image by using the encoder and decoder networks respectively. The autoencoder group consists of several encoders and decoders. The principle of the form of the sub-network is as follows: The generator G reads the input image x, where x $\in R^{w \times h \times c}$, and forwards it to its encoder network G_E. By using convolutional layers, batch-norm and leaky ReLU() activation, G_E compresses x into a vector z to reduce the size of x, where $z \in R^d$.

Number of convolutional/transposed convolution is:

$$m2 = \frac{\dim(x)}{16} + k2, \, k2 = 0, 1, 2, \ldots, n \tag{3}$$

The latent representation z of x is also called bottleneck features of G. When the model training is completed, z can be considered as the best feature representation of x and has the smallest dimension. The decoder part G_D of the generator network G adopts an architecture similar to the generator in DCGAN [58], which includes the deconvolution layer, ReLU() activation, batch-norm and tanh layer. G_D reconstructs the vector z into $\hat{x}$, where $\hat{x} \in R^{w \times h \times c}$, which has the same dimension as x. The autoencoder group performs multiple reconstruction processes according to the number of autoencoders, so that the model increases the reconstruction difference of abnormal samples. In summary, the self-encoder

group DE generates an image $\hat{x}$ through multiple $\hat{x} = G_{D_i}(z)$ processes, where $z = G_{E_i}(x)$.

The second sub-network is the encoder network E, which compresses the image $\hat{x}$ output from the encoder group DE into $\hat{z}$, where $\hat{z}$ and z have the same dimensions. Through different parameterization, it has the same architecture as G_E. E process the compression process of $\hat{x}$ as $\hat{z} = E(\hat{x})$, and $\hat{z}$ is the characteristic representation of $\hat{x}$. In order to calculate the reconstruction difference more conveniently in the anomaly detection stage, the dimension of the vector $\hat{z}$ is the same as the dimension of z. Subnet E is the most unique part of this model. Different from the existing methods based on autoencoders, in this method, the bottleneck features are used to minimize the potential vector. After the model has been fully trained, the subnet E minimize the distance by parameterization. In addition, in the testing phase, anomaly detection is performed through this minimized distance.

The third sub-network is the discriminator network D. Its function is to distinguish between input x and output $\hat{x}$, and mark them as real samples or fake samples respectively. This subnet is the standard discriminator network introduced in DCGAN [58].

B. MODEL TRAINING

The principle of self-adaption AAE-GAN model anomaly detection is as follows: In the training phase of the model, only normal samples are used for parameter optimization. In the anomaly detection phase, the abnormal samples x are input into the generator network G, due to no abnormal samples are involved in the training process, G_E cannot map the input x to the latent representation z well, and G_D also cannot reconstruct the abnormal samples well. The primary cause is that the parameters in G_E and G_D are not suitable for processing reconstruction of abnormal samples. The output result $\hat{x}$ of the autoencoder group DE also causes the encoder network E to be incorrectly mapped to the abnormal feature representation $\hat{z}$, which increases the difference between z and $\hat{z}$. When this difference is obvious, the model will treat the sample x as an abnormal sample. In order to make the reconstruction difference of the abnormal samples more significant, this paper uses the autoencoder group to encode and decode the samples, so that the reconstruction difference of the abnormal samples is significantly enlarged. In order to verify this hypothesis, we formulate the objective function by combining three loss functions, each of which plays an important role in the optimization of the network architecture.

1) STRUGGLE-LOSS

In order to reduce the instability of GAN in the training process, we adopt the feature matching loss proposed by Salimans *et al.* [60]. In the GAN model proposed by Goodfellow *et al.*, both the generator G and the discriminator D need to be optimized through the output results of the discriminator D, which will reduce the stability of the GAN training process. In our model, the generator G updates the parameters according to the intermediate representation

of the discriminator D. Specifically, given an input x that conforms to the data distribution p_X, suppose a function f is used as the middle layer of the discriminator D. We use the idea of feature matching to calculate the L2 distance between the original feature image and the generated image. Therefore, our Struggle-loss L_{str} is defined as:

$$L_{str} = E_{x \sim p_X} \left\| f(x) - E_{x \sim p_X} f(G(x)) \right\|_2 \quad (4)$$

2) CONTEXT-LOSS

After having the Struggle-loss L_{str}, we can fully train the discriminator D, but the generator G cannot optimize the parameters based on the input samples. We refer to the method proposed by Isola et al. [59] to train the generator G through the L1 distance between the input sample and the generated sample. Since Isola et al. pointed out that the result produced by using the L1 distance is better than the L2 distance, so we also use the L1 distance. Therefore, we also use the context-loss L_{con} to train G by measuring the L1 distance between the original x and the generated image ($\hat{x} = G(x)$), where $\hat{x}$ takes the value of the last decoder in the encoder group Output result:

$$L_{con} = E_{x \sim p_X} \left\| x - G(x) \right\|_1 \quad (5)$$

3) ENCODER-LOSS

The two loss functions mentioned above can make the reconstructed samples generated by the generator not only be close to the original samples, but also have a reasonable context. In addition, we added an additional encoder loss function L_{enc}, its goal is to minimize the potential features of the input sample ($z = G_E(x)$) and the potential features of the generated sample ($\hat{z} = E(G(x))$), where $\hat{z}$ is the final output result of the generator network. The formal definition of L_{enc} is:

$$L_{enc} = E_{x \sim p_X} \left\| G_E(x) - E(G(x)) \right\|_2 \quad (6)$$

In summary, the generator learns how to perform feature encoding on the input normal samples through a series of encoding and decoding operations. However, in the case of input abnormal samples, since both the DE and E networks are only optimized for normal samples, the distance between x and $\hat{x}$ and z and $\hat{z}$ cannot be minimized. In summary, our objective function for the generator is as follows:

$$L = w_{str} L_{str} + w_{con} L_{con} + w_{enc} L_{enc} \quad (7)$$

w_{str}, w_{con} and w_{enc} are weighted parameters that adjust the influence of a single loss on the overall objective function. We set them all to 1/3.

C. ANOMALY SCORE

In the testing phase, the model uses the weighted average of L_{con} and L_{enc} given in (5) and (6) to score anomalies in a given image. Therefore, for the test sample $\hat{x}$, our anomaly score $A(\hat{x})$ or $s_{\hat{x}}$ is defined as:

$$A(\hat{x}) = w_1 L_{con} + w_2 L_{enc} \quad (8)$$

TABLE 2. The influence of threshold ε on model performance.

ε	0.1	0.2	0.3	0.4	0.5	0.6	0.7	0.8
Precision	0.582	0.667	0.721	0.862	0.876	0.948	1.0	1.0
F1_score	0.735	0.781	0.749	0.831	0.530	0.258	0.109	0.063

In order to facilitate our evaluation of the model anomaly detection performance, we have prepared a test set $\acute{D}$, and calculated the anomaly score of each test sample $\hat{x}$ in the test set according to (8), and finally formed a set of abnormal scores $S = \{s_i : A(\acute{x}_i), \acute{x}_i \in \acute{D}\}$. In order to facilitate comparison and statistics, we use feature scaling technology to scale each score to the range of [0, 1], the formula is as follows:

$$\acute{s}_i = \frac{s_i - \min(S)}{\max(S) - \min(S)} \quad (9)$$

Equation 9 finally generates an anomaly score vector $\acute{S}$ for the final evaluation of the test set. If $\acute{s}_i$ is greater than a threshold ε, we consider this sample to be an abnormal sample. The setting of the threshold ε will directly affect the accuracy of model detection. The specific conditions are as follows:

Algorithm 1 Anomaly Detection Algorithm Used the Self-Adaption AAE-GAN

Input: training data X_{train}, testing data X_{test}
Output: anomaly or no anomaly
At training model stage:
    Initialize Gen, Dis
    In each iteration:
        Generate random mini-batch X from training data X_{train}
        Generate z from encoder $z = G_{E_i}(x)$
        Generate $\hat{x}$ from decoder $\hat{x} = G_{D_i}(z)$
        Generate $\hat{z}$ from decoder $\hat{z} = E(\hat{x})$
        Update parameters of discriminator according to gradient

$$\theta_{Dis} \leftarrow \left\{ E_{x \sim X_{train}} \left\| f(x) - E_{x \sim p_X} f(G(x)) \right\|_2 \right\}_{Dis}$$

        Update parameters of generator according to gradient

$$\theta_{Gen} \leftarrow \left\{ E_{x \sim X_{train}} \left\| x - G(x) \right\|_1 \right\}_{Gen}$$

        Update parameters of encoder according to gradient

$$\theta_E \leftarrow \left\{ E_{x \sim X_{train}} \left\| G_E(x) - E(G(x)) \right\|_2 \right\}_E$$

At anomaly detection stage:
    Calculate L_{con}: $E_{x \sim X_{test}} \left\| x - G(x) \right\|_1$
    Calculate L_{enc}: $E_{x \sim X_{test}} \left\| G_E(x) - E(G(x)) \right\|_2$
    Calculate anomaly score: $A(x_{test}) = w_1 L_{con} + w_2 L_{enc}$
    Calculate anomaly score for each point of the testing data X_{test}
    if (score > threshold):
        return anomaly
    else:
    return no anomaly

IV. EXPERIMENTAL RESULT

A. TIME SERIES DATA

A time series is a sequence of data points arranged in the order of time. In other words, it is a sequence composed of consecutive points at equal intervals in time.

We use three time series datasets in the experiment. They are aluminum electrolysis industry data, SWaT and WADI,

which are used to evaluate the performance of the time series anomaly detection model in this paper. In these datasets, both abnormal and normal points need to be marked. The introduction of each dataset is as follows:

SWaT: The Safe Water Treatment (SWaT) system is an operational test platform for water treatment that represents the working process of a large modern water treatment plant in a large city [67]. The overall design of the test platform was done in collaboration with the Public Utilities Commission of Singapore, the national water utility, to ensure that the overall physical processes and control systems were similar to the real systems on site. The SWaT dataset collection process lasted 11 days, with the system running 24 hours a day. In the last four days of the 2016 SWaT data collection process, a total of 36 attacks were launched. Typically, targets of attack include sensors (e.g., water level sensors, flow rate counters, etc.) and brakes (e.g., valves, pumps, etc.). Over the last four days, these attacks were launched on the test platform with different intents and durations ranging from a few minutes to an hour. Allowing the system to reach its normal operational state before another attack or before successive attacks were launched. For more detailed information about SWaT dataset, visit the SWaT Website.

The water purification process in SWaT consists of six sub-processes, called P1 through P6. The first process is about raw water supply and storage, and P2 is a pretreatment used to assess water quality. Undesired components are removed by backwashing with an ultrafiltration unit (UF) in P3. The excess chlorine is removed in the fourth process (P4). The water from the P4 is then pumped into the reverse osmosis (RO) system (P5) to reduce inorganic impurities. Finally, P6 stores water ready for distribution.

WADI: Unlike the water treatment system plant, which is usually located in a fixed location, the water supply system consists of numerous pipes spanning a large area. This greatly increases the risk of a physical attack on the water supply network. The Water Distribution (WADI) [68] test platform is an extension of the SWaT system that absorbs a portion of SWaT reverse osmosis permeate and raw water to form a complete and realistic water treatment system, a storage and distribution network. There are three control processes in the water supply system. The first process is to obtain raw water from SWaT, PUB inlet or WADI return water and store raw water in two tanks. P2 distributes water from two elevated tanks and six consumer tanks according to preset demand patterns. The water is recycled and returned to P1 in the third step.

The WADI test platform is also equipped with a quantitative chemical feed system, booster pumps, valves, instruments and analyzers. In addition to network simulation of attack and defense on a PLC, WADI also has the capability to simulate the effects of physical attacks such as water leaks and malicious chemical injections. The WADI data collection process consists of 16 consecutive days of operations, of which 14 days are collected under normal operation and 2 days are collected in the event of an attack. During the data

collection, all network data, sensor and actuator data were collected. For more details on the WADI data set, visit the WADI website.

Aluminum electrolysis data: The aluminum electrolysis data in this article comes from certain Intelligent Technology Company. The first phase of the ''data service platform'' construction project of China Aluminum Technology Center was started in December 2017 and had been completed as of January 2019 Data collection of 5 production companies in 3 sectors: electrolytic aluminum sector (Huasheng, Shanxi New Materials, Lanzhou), alumina sector (Guangxi, Zunyi), carbon sector (Shanxi New Materials). The carbon and alumina are the anode and electrolyte in the aluminum electrolysis process. We focus on the state of the aluminum electrolysis cell in the aluminum electrolysis process. In the process of aluminum electrolysis, both alumina and carbon are consumed, resulting in parameters such as alumina concentration. We comprehensively judge whether the aluminum electrolysis cell is abnormal based on these parameters. The aluminum electrolysis data includes 203 parameters, and each parameter takes a value once a day.

As the energy consumption of upstream and downstream products of aluminum electrolysis and the consumption of raw materials have increased significantly, the technical indicators have deteriorated, and the product quality has also declined; the comprehensive energy consumption and the process energy consumption have increased significantly. Production departments are very concerned about the changes in key indicators, including energy consumption indicators such as water, gas, wind, and electricity, and controllable production data indicators for electrolytic aluminum. Due to the many key indicators related to the upstream and downstream of electrolytic aluminum, the organization and management of production operation are quite difficult, the adjustment and optimization measures of production operation are relatively lagging, and the control of production costs is very difficult. It is necessary to optimize the existing production operation control mode and cost management mode.

Collect and sort out the production data of the electrolytic aluminum plate, and monitor the key indicators, and study the changes of the key indicator data, the decision-making methods, and the relationship between the key indicators. Carry out layer-by-layer decomposition, study the relationship between process consumption and main technical indicators and their interactions, find out various factors that affect key indicators through empirical formulas, data mining algorithms, statistical analysis and other methods, and establish key indicators and main technical indicators mathematical model. In order to ensure the implementation effect of the key indicator models of electrolytic aluminum, the achievement of various operating indicators should be dynamically monitored to ensure that the results of production process control will be reflected in operating performance. The total number of collected data is 280,000, and there are 203 parameters involved. The details are shown in Table 3:
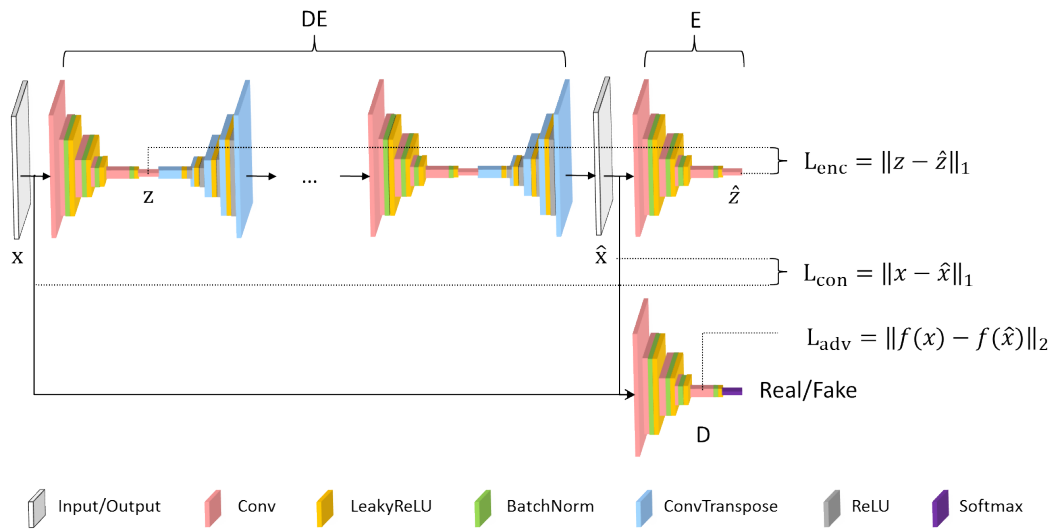
FIGURE 1. Self-adaption AAE-GAN.

TABLE 3. General information about datasets.

Item	SWaT	WADI	Aluminum electrolysis
Variables	51	103	203
Training size (normal data)	496800	1048571	210000
Testing size (data with attacks)	449919	172801	70000
N_rate(%)	88.02	94.01	89.01
N_rate is the proportion of normal data points in the test set to all test datasets			

Due to the variety of data in aluminum electrolysis cells, it is difficult for experts to assess the status of data samples. In order to facilitate the labeling of aluminum electrolysis experts, in the field of aluminum electrolysis we have proposed an automatic sample labeling method to assist experts in marking samples. The labeling system requires experts to provide the following parameters: labeling parameters, the number of consecutive samples of the labeling parameters, and the number of samples with abnormal trends forwarded. The labeling parameter is used to label the sample, and the normal range of the labeling parameter needs to be given, and the sample is divided into three states: normal, abnormal trend, and abnormal. The number of consecutive samples of labeling parameter n is used to label abnormal samples, and the average value of n continuous samples is compared with the normal range of the labeled parameter. If the range is exceeded, it is judged as abnormal; the number of samples with abnormal trend forwarded m is used to label abnormal trend, the abnormal sample is pushed forward by m days, this m days is the abnormal trend sample. The network model mainly learns abnormal trend samples that cannot be distinguished by experts. The abnormal trend samples and abnormal samples are collectively called abnormal samples.

B. DATA PREPROCESSING

In data preprocessing, in order to minimize the computational burden of self-adaption AAE-GAN, we use PCA to project the original multivariate time series data into the lower-dimensional space, instead of directly inputting the high-dimensional data to self-adaption AAE-GAN model. In this paper, we set the value of PC to 25. Then, in order to use the ability of GAN to learn complex high-dimensional image distributions, we convert the reduced-dimensional multi-dimensional time series data into a two-dimensional matrix. Since there are many parameters of aluminum electrolysis, in order to make the data points of each two-dimensional matrix evenly distributed, we calculate the maximum value max and minimum value min of each parameter, so that the upper and lower limits of each time series curve are equal to 0.9*max and 1.1*min. Each curve represents a parameter.

In addition, in some industrial productions, such as the aluminum electrolysis industry, it is usually impossible to determine whether the aluminum electrolysis cell has abnormalities based on the values of various sensors during one day. It is necessary to obtain the values of various parameters in multiple time steps to determine whether there are abnormalities. If the molecular ratio and voltage of a certain electrolytic cell on one day are too large or too small, it cannot be judged that the electrolytic cell on that day is abnormal. In addition, there are serious hysteresis problems in the aluminum electrolysis industry. For example, an expert adjusts the temperature of an electrolysis cell on a certain day, but the expert does not know whether it is correct or not. You must observe the state of each parameter in a later period of time to judge. And, there are usually many states that experts cannot distinguish. Therefore, we divide the data into segments, and divide the multivariate time series into multiple sub-sequences through a sliding window with a size of 10 and step 2 for the training phase and the testing phase. The final result is shown in Fig. 2:

This experimental result shows the result of converting a multi-dimensional time series into a two-dimensional matrix. The x axis of the image represents time, the y axis represents
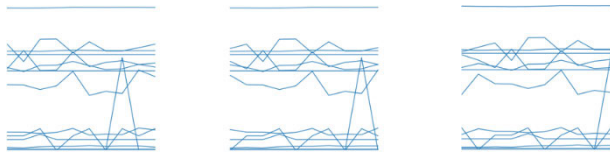
FIGURE 2. Data preprocessing results.

the value of each parameter, and each curve represents the trend of a parameter over time. At this point, we focus on the trend of each curve, not on the parameter that each curve represents. Three images show the process of cutting the sample, cutting multi-dimensional time series in a step.

If a certain two-dimensional matrix contains abnormal sample data, then we divide this matrix into abnormal samples, other matrices are divided into normal samples, and therefore the generated two-dimensional matrix sample is divided into two parts. Since our model only learns on the distribution of normal data during the model training phase, our first part of the data does not contain any abnormal samples. The data in the second part contains normal and abnormal samples for model testing.

C. EVALUATION CRITERIA AND RESULTS

We use Precision, Roc and F1 scores to evaluate the anomaly detection performance of our model.

$$\text{Precision} = \frac{TP}{TP + FP} \tag{10}$$

$$\text{Recall} = \frac{TP}{TP + FN} \tag{11}$$

$$\text{F1} = \frac{2 \times \text{Precision} \times \text{Recall}}{\text{Precision} + \text{Recall}} \tag{12}$$

where TP is the number that is correctly detected in all normal points, FP is the number that is detected as abnormal in all normal points, and FN is the number that is detected as normal in all abnormal points.

The full name of ROC is Receiver Operating Characteristic Curve. As the name suggests, its main function is to analyze the problem by drawing this characteristic curve. The ROC curve defines the false positive rate (FPR) as the X axis and the true positive rate (TPR) as the Y axis. The formula for calculating these two values is as follows:

1) TPR

In all samples that are actually normal, the rate that is correctly detected as normal.

$$\text{TPR} = \frac{TP}{TP + FN} \tag{13}$$

2) FPR

In all samples that are actually abnormal, the ratio of falsely detected as normal.

$$\text{FPR} = \frac{FP}{FP + TN} \tag{14}$$

Put in specific areas to understand the above two indicators. For example, in the electrolytic cell abnormality detection, expert want to determine the abnormal electrolytic cell. Then try to identify the real normal samples, that is, the first indicator TPR, the higher the better. Try to identify what is really abnormal, that is, the second indicator FPR, the lower the better. It is not difficult to find that these two indicators influence each other. If an expert's judgment on abnormal symptoms is rather vague, and basically regards all samples as normal, then his first index should be very high, but the second index will be correspondingly higher. In the most extreme case, he regards all electrolytic cell as normal, then the first index reaches 1, and the second index is also 1.

The value of AUC is the area covered by the ROC curve. Obviously, the larger the AUC, the better the classification effect of the classifier will be. When AUC = 1, it can be proved that this is a perfect classifier. When using this model to predict samples, no matter what threshold is set, the correct prediction can be obtained. But in most practical situations, a perfect classifier is impossible. When $0.5 < \text{AUC} < 1$, it proves that this classifier is better than random guessing. This classifier (model) can get good prediction results if the threshold is properly set. When AUC = 0.5, the effect of this classifier is the same as the random guessing (for example: toss a coin), which proves that this model has no application value. When AUC <0.5, the effect of this model is worse than random guessing; but as long as you always make backward predictions, you will get better results than random guessing. Our experiment mainly records the value of AUC in the ROC curve.

In order to evaluate the performance of this method, we implemented three baseline methods, which are representative time series anomaly detection methods based on generative models and sample reconstruction. They all perform anomaly detection by reconstructing the difference.

Table 4 shows the final results of our self-adaption AAE-GAN method based on adaptively changing according to the input samples, and the final results of the representative time series anomaly detection method based on the generative model. Both LSTM-AE and LSTM-VAE use the LSTM network as the basic module, and the values of the parameters are the same as those in the LSTM-based VAE-GAN. In order to compare the anomaly detection capabilities of the model more objectively, we use the same threshold, window length, and moving step selection strategy for all methods. As shown in Table 4, compared to other generative models, our method does not perform very well in SWaT and WADI which are based on a single point of data to identify abnormal dataset. However, in the field of aluminum electrolysis, it is necessary to determine whether an abnormality occurs during this period based on the time series data at multiple time steps. The performance of our model is higher than the existing time series anomaly detection method based on the generative model.

Table 5 shows the final results of our self-adaption AAE-GAN method based on adaptive changes according

TABLE 4. Generate model comparison results.

Dataset	Method	Roc	Precision	F1 _score
SWaT	LSTM-AE	0.443	0.430	0.572
	LSTM-VAE	0.822	0.820	0.720
	self-adaption AAE-GAN	0.512	0.575	0.475
WADI	LSTM-AE	0.350	0.361	0.260
	LSTM-VAE	0.205	0.213	0.320
	self-adaption AAE-GAN	0.251	0.249	0.224
Aluminum electrolysis	LSTM-AE	0.781	0.772	0.750
	LSTM-VAE	0.322	0.220	0.321
	self-adaption AAE-GAN	0.851	0.862	0.831

TABLE 5. Methods based sample reconstruction comparison results.

Dataset	Method	Roc	Precision	F1 _score
SWaT	MAD-GAN	0.978	0.985	0.700
	GANomaly	0.272	0.318	0.265
	self-adaption AAE-GAN	0.512	0.575	0.475
WADI	MAD-GAN	0.441	0.469	0.322
	GANomaly	0.226	0.211	0.212
	self-adaption AAE-GAN	0.251	0.249	0.224
Aluminum electrolysis	MAD-GAN	0.681	0.602	0.550
	GANomaly	0.812	0.753	0.632
	self-adaption AAE-GAN	0.851	0.862	0.831

to the input samples, and the final results of representative time series anomaly detection methods based on the idea of sample reconstruction. MAD-GAN uses the LSTM network as the basic module, and the values of the parameters are the same as those in the LSTM-based VAE-GAN. GANomaly uses the GAN network as the basic module, and its basic parameters are similar to those in DCGAN. We also use the same threshold, window length and moving step selection strategy for all methods. As shown in Table 5, compared to other anomaly detection models based on the idea of sample reconstruction, our method also performs poorly on SWaT and WADI datasets, but in the field of aluminum electrolysis, our model performs better than the existing ones based on time series anomaly detection method which was based on the idea of sample reconstruction.

V. CONCLUSION

In this paper, a time series anomaly detection method named the self-adaption AAE-GAN based on the adaptive change according to the input samples is proposed. This method aims to judge whether the equipment is abnormal through the aluminum reduction cell data collected in the form of time series.

The time series anomaly detection method based on sample reconstruction can be divided into two stages. One is the model training stage, where the model learns the distribution of normal data. The other is the anomaly detection stage, where anomaly scores of the time series are calculated to identify anomalies. The self-adaption AAE-GAN joint training generator and discriminator can utilize the mapping capabilities of the encoder and decoder at the same time. Meanwhile, the optimization process in the anomaly detection phase is avoided, so that anomalies can be detected faster and more accurately. In experiments based on SWaT, WADI and aluminum electrolysis time series data, our method has an higher performance on aluminum electrolysis dataset than other time series anomaly detection methods based on generative models and sample reconstruction. Our model is suitable for specific industrial scenarios, such as the aluminum electrolysis industry. Experts will not need to pay special attention to whether there is an abnormality on a certain day, because it is very difficult and not rigorous to judge the state of the aluminum electrolysis cell on a certain day. It is necessary to observe a certain period to judge whether the state of the aluminum electrolytic cell is abnormal. For industrial scenarios that only focus on the state of the equipment on a certain day, our model cannot achieve the optimal results. Due to the moving window mechanism, the anomaly scores of certain points are calculated multiple times, but the accuracy is not affected by the number of calculations of the anomaly scores in the anomaly detection stage. In order to increase the number of samples used to train the model in the training phase, we usually set the step size to be smaller than the length of the window. If the length of the time series is long enough, the time series can be divided by the length of the window as the time interval.

Although our method can accurately and quickly detect anomalies in time series, it still has some limitations. In our paper, we judge whether there is an abnormality during this period of time based on the time series data of multiple time steps, and the threshold and window size of the abnormality score are designed according to the aluminum electrolysis background. In certain scenarios where the abnormal state at a specific point in time needs to be known, a new abnormal scoring mechanism design is required to meet this application scenario.

Our research has room for further development. In the current situation, our method needs to try certain data to adjust the threshold and window length of the abnormal score. Our next improvement goal is to provide an adaptive threshold and window adjustment method that can speed up the model training time.

REFERENCES

[1] M. O. Gokalp, K. Kayabay, M. A. Akyol, P. E. Eren, and A. Kocyigit, "Big data for industry 4.0: A conceptual framework," in *Proc. Int. Conf. Comput. Sci. Comput. Intell. (CSCI)*, Dec. 2016, pp. 431–434, doi: 10.1109/CSCI.2016.0088.

[2] M. Marjani, F. Nasaruddin, A. Gani, A. Karim, I. A. T. Hashem, A. Siddiqa, and I. Yaqoob, "Big IoT data analytics: Architecture, opportunities, and open research challenges," *IEEE Access*, vol. 2017, 5, pp. 5247–5261.

[3] L. Martí, N. Sanchez-Pi, J. Molina, and A. Garcia, "Anomaly detection based on sensor data in petroleum industry applications," *Sensors*, vol. 15, no. 2, pp. 2774–2797, Jan. 2015.

[4] C. Gao, Y. Chen, Z. Wang, H. Xia, and N. Lv, "Anomaly detection frameworks for outlier and pattern anomaly of time series in wireless sensor networks," in *Proc. Int. Conf. Netw. Netw. Appl. (NaNA)*, Dec. 2020, pp. 229–232, doi: 10.1109/NaNA51271.2020.00046.

[5] L. von Werra, L. Tunstall, and S. Hofer, "Unsupervised anomaly detection for seasonal time series," in *Proc. 6th Swiss Conf. Data Sci. (SDS)*, Jun. 2019, pp. 136–137, doi: 10.1109/SDS.2019.00036.

[6] Y. Qin and Y. Lou, "Hydrological time series anomaly pattern detection based on isolation forest," in *Proc. IEEE 3rd Inf. Technol., Netw., Electron. Autom. Control Conf. (ITNEC)*, Mar. 2019, pp. 1706–1710, doi: 10.1109/ITNEC.2019.8729405.

[7] Z. Zhao, Y. Zhang, X. Zhu, and J. Zuo, "Research on time series anomaly detection algorithm and application," in *Proc. IEEE 4th Adv. Inf. Technol., Electron. Autom. Control Conf. (IAEAC)*, Dec. 2019, pp. 16–20, doi: 10.1109/IAEAC47372.2019.8997819.

[8] C. C. Aggarwal and P. S. Yu, "Outlier detection for high dimensional data," in *Proc. ACM SIGMOD Int. Conf. Manage. Data*, Santa Barbara, CA, USA, May 2001, pp. 37–46.

[9] C. C. Aggarwal and P. S. Yu, "Outlier detection with uncertain data," in *Proc. SIAM Int. Conf. Data Mining*, Atlanta, GA, USA, Apr. 2008, pp. 483–493.

[10] C. C. Aggarwal, "On abnormality detection in spuriously populated data streams," in *Proc. SIAM Int. Conf. Data Mining*, Newport Beach, CA, USA, Apr. 2005, pp. 80–91.

[11] C. C. Aggarwal, Y. Zhao, and P. S. Yu, "Outlier detection in graph streams," in *Proc. IEEE 27th Int. Conf. Data Eng.*, Hannover, Germany, Apr. 2011, pp. 399–409.

[12] J. Gao, F. Liang, W. Fan, C. Wang, Y. Sun, and J. Han, "On community outliers and their efficient detection in information networks," in *Proc. 16th ACM SIGKDD Int. Conf. Knowl. Discovery Data Mining*, Washington, DC, USA, Jul. 2010, pp. 813–822.

[13] R. Chalapathy and S. Chawla, "Deep learning for anomaly detection: A survey," 2019, *arXiv:1901.03407*. [Online]. Available: http://arxiv.org/abs/1901.03407

[14] R. J. B. J. Pincus, V. Barnett, and T. Lewis, *Outliers in Statistical Data*. Hoboken, NJ, USA: Wiley, 1994, pp. 199–256.

[15] J. Contreras, R. Espinola, F. J. Nogales, and A. J. Conejo, "ARIMA models to predict next-day electricity prices," *IEEE Trans. Power Syst.*, vol. 18, no. 3, pp. 1014–1020, Aug. 2003.

[16] P. J. Rousseeuw and A. M. Leroy, *Robust Regression and Outlier Detection*. Hoboken, NJ, USA: Wiley, 2005.

[17] P. Baraldi, L. Podofillini, L. Mkrtchyan, E. Zio, and V. N. Dang, "Comparing the treatment of uncertainty in Bayesian networks and fuzzy expert systems used for a human reliability analysis application," *Rel. Eng. Syst. Saf.*, vol. 138, pp. 176–193, Jun. 2015.

[18] V. Vapnik, *The Nature of Statistical Learning Theory*. New York, NY, USA: Springer, 2013.

[19] T. Han, D. Jiang, Q. Zhao, L. Wang, and K. Yin, "Comparison of random forest, artificial neural networks and support vector machine for intelligent diagnosis of rotating machinery," *Trans. Inst. Meas. Control*, vol. 40, no. 8, pp. 2681–2693, May 2018.

[20] S. Haykin, *Neural Networks: A Comprehensive Foundation*. Upper Saddle River, NJ, USA: Prentice-Hall, 1994.

[21] Y. Lei, F. Jia, J. Lin, S. Xing, and S. X. Ding, "An intelligent fault diagnosis method using unsupervised feature learning towards mechanical big data," *IEEE Trans. Ind. Electron.*, vol. 63, no. 5, pp. 3137–3147, May 2016.

[22] H. Yin and K. Gai, "An empirical study on preprocessing high-dimensional class-imbalanced data for classification," in *Proc. IEEE IEEE 17th Int. Conf. High Perform. Comput. Commun. 7th Int. Symp. Cyberspace Saf. Secur., IEEE 12th Int. Conf. Embedded Softw. Syst.*, Aug. 2015, pp. 1314–1319.

[23] S. N. Kalid, K.-H. Ng, G.-K. Tong, and K.-C. Khor, "A multiple classifiers system for anomaly detection in credit card data with unbalanced and overlapped classes," *IEEE Access*, vol. 8, pp. 28210–28221, 2020, doi: 10.1109/ACCESS.2020.2972009.

[24] J. Pereira and F. Saraiva, "A comparative analysis of unbalanced data handling techniques for machine learning algorithms to electricity theft detection," in *Proc. IEEE Congr. Evol. Comput. (CEC)*, Jul. 2020, pp. 1–8, doi: 10.1109/CEC48606.2020.9185822.

[25] L. Bontemps, J. McDermott, and N.-A. Le-Khac, "Collective anomaly detection based on long short-term memory recurrent neural networks," in *Proc. Int. Conf. Future Data Secur. Eng.*, Can Tho City, Vietnam, Nov. 2016, pp. 141–152.

[26] K. Hundman, V. Constantinou, C. Laporte, I. Colwell, and T. Soderstrom, "Detecting spacecraft anomalies using LSTMs and nonparametric dynamic thresholding," in *Proc. 24th ACM SIGKDD Int. Conf. Knowl. Discovery Data Mining*, London, U.K., Jul. 2018, pp. 387–395.

[27] S. Chauhan and L. Vig, "Anomaly detection in ECG time signals via deep long short-term memory networks," in *Proc. IEEE Int. Conf. Data Sci. Adv. Analytics (DSAA)*, Paris, France, Oct. 2015, pp. 1–7.

[28] P. Malhotra, L. Vig, G. Shroff, and P. Agarwal, "Long short term memory networks for anomaly detection in time series," in *Proc. 23rd Eur. Symp. Artif. Neural Netw., Comput. Intell. Mach. Learn.*, Bruges, Belgium, Apr. 2015, pp. 89–94.

[29] D. Park, Y. Hoshi, and C. C. Kemp, "A multimodal anomaly detector for robot-assisted feeding using an LSTM-based variational autoencoder," *IEEE Robot. Autom. Lett.*, vol. 3, no. 3, pp. 1544–1551, Jul. 2018.

[30] C. Zhang, D. Song, Y. Chen, X. Feng, C. Lumezanu, W. Cheng, J. Ni, B. Zong, H. Chen, and N. V. Chawla, "A deep neural network for unsupervised anomaly detection and diagnosis in multivariate time series data," in *Proc. AAAI Conf. Artif. Intell.*, Palo Alto, CA, USA, Feb. 2019, pp. 1409–1416.

[31] B. Zong, Q. Song, M. R. Min, W. Cheng, C. Lumezanu, D. Cho, and H. Chen, "Deep autoencoding Gaussian mixture model for unsupervised anomaly detection," in *Proc. 6th Int. Conf. Learn. Represent.*, Vancouver, BC, Canada, Apr./May 2018. [Online]. Available: https://openreview.net/forum?id=BJJLHbb0-

[32] Y. Guo, W. Liao, Q. Wang, L. Yu, T. Ji, and P. Li, "Multidimensional time series anomaly detection: A gru-based Gaussian mixture variational autoencoder approach," in *Proc. Asian Conf. Mach. Learn.*, Bejing, China, Nov. 2018, pp. 97–112.

[33] R.-Q. Chen, G.-H. Shi, W.-L. Zhao, and C.-H. Liang, "A joint model for IT operation series prediction and anomaly detection," 2019, *arXiv:1910.03818*. [Online]. Available: http://arxiv.org/abs/1910.03818

[34] P. Malhotra, A. Ramakrishnan, G. Anand, L. Vig, P. Agarwal, and G. Shroff, "LSTM-based encoder-decoder for multi-sensor anomaly detection," 2016, *arXiv:1607.00148*. [Online]. Available: http://arxiv.org/abs/1607.00148

[35] I. Goodfellow, J. Pouget-Abadie, M. Mirza, B. Xu, D. Warde-Farley, S. Ozair, A. Courville, and Y. Bengio, "Generative adversarial nets," in *Proc. Adv. Neural Inf. Process. Syst.*, 2014, pp. 2672–2680.

[36] T. Schlegl, P. Seeböck, S. M. Waldstein, U. Schmidt-Erfurth, and G. Langs, "Unsupervised anomaly detection with generative adversarial networks to guide marker discovery," in *Proc. Int. Conf. Inf. Process. Med. Imag.* New York, NY, USA: Springer, 2017, pp. 146–157.

[37] J. Donahue, P. Krähenbühl, and T. Darrell, "Adversarial feature learning," 2016, *arXiv:1605.09782*. [Online]. Available: http://arxiv.org/abs/1605.09782

[38] S. Akcay, A. Atapour-Abarghouei, and T. P. Breckon, "GANomaly: Semi-supervised anomaly detection via adversarial training," 2018, *arXiv:1805.06725*. [Online]. Available: http://arxiv.org/abs/1805.06725

[39] J. Liu, F. Qu, X. Hong, and H. Zhang, "A small-sample wind turbine fault detection method with synthetic fault data using generative adversarial nets," *IEEE Trans. Ind. Informat.*, vol. 15, no. 7, pp. 3877–3888, Jul. 2019.

[40] T. Han, C. Liu, W. Yang, and D. Jiang, "A novel adversarial learning framework in deep convolutional neural network for intelligent diagnosis of mechanical faults," *Knowl.-Based Syst.*, vol. 165, pp. 474–487, Feb. 2019.

[41] W. Mao, Y. Liu, L. Ding, and Y. Li, "Imbalanced fault diagnosis of rolling bearing based on generative adversarial network: A comparative study," *IEEE Access*, vol. 7, pp. 9515–9530, 2019.

[42] D. Li, D. Chen, J. Goh, and S.-K. Ng, "Anomaly detection with generative adversarial networks for multivariate time series," 2018, *arXiv:1809.04758*. [Online]. Available: http://arxiv.org/abs/1809.04758

[43] D. Li, D. Chen, B. Jin, L. Shi, J. Goh, and S. K. Ng, "MAD-GAN: Multivariate anomaly detection for time series data with generative adversarial networks," in *Proc. 28th Int. Conf. Artif. Neural Netw.*, Munich, Germany, Sep. 2019, pp. 703–716.

[44] C. Cheng, G. Ma, Y. Zhang, M. Sun, F. Teng, H. Ding, and Y. Yuan, "Online bearing remaining useful life prediction based on a novel degradation indicator and convolutional neural networks," 2018, *arXiv:1812.03315*. [Online]. Available: http://arxiv.org/abs/1812.03315

[45] A. Taylor, S. Leblanc, and N. Japkowicz, "Anomaly detection in automobile control network data with long short-term memory networks," in *Proc. IEEE Int. Conf. Data Sci. Adv. Analytics (DSAA)*, Oct. 2016, Art. no. 130139.

[46] T. Guo, Z. Xu, X. Yao, H. Chen, K. Aberer, and K. Funaya, "Robust online time series prediction with recurrent neural networks," in *Proc. IEEE Int. Conf. Data Sci. Adv. Anal. (DSAA)*, Oct. 2016, Art. no. 816825.

[47] S. Kanarachos, S.-R. G. Christopoulos, A. Chroneos, and M. E. Fitzpatrick, "Detecting anomalies in time series data via a deep learning algorithm combining wavelets, neural networks and Hilbert transform," *Expert Syst. Appl.*, vol. 85, Nov. 2017, Art. no. 292304.

[48] K. Veeramachaneni, I. Arnaldo, V. Korrapati, C. Bassias, and K. Li, "Ai²: Training a big data machine to defend," in *Proc. IEEE 2nd Int. Conf. Big Data Secur. Cloud (BigDataSecurity), IEEE Int. Conf. High Perform. Smart Comput. (HPSC), IEEE Int. Conf. Intell. Data Secur. (IDS)*, Apr. 2016, p. 4954.

[49] Z. Wu, W. Lin, and Y. Ji, "An integrated ensemble learning model for imbalanced fault diagnostics and prognostics," *IEEE Access*, vol. 6, 2018, Art. no. 83948402.

[50] M. Galar, A. Fernandez, E. Barrenechea, H. Bustince, and F. Herrera, "A review on ensembles for the class imbalance problem: Bagging-, boosting-, and hybrid-based approaches," *IEEE Trans. Syst., Man, Cybern. C, Appl. Rev.*, vol. 42, no. 4, Jul. 2012, Art. no. 463484.

[51] N. V. Chawla, K. W. Bowyer, L. O. Hall, and P. W. Kegelmeyer, "SMOTE: Synthetic minority over-sampling technique," *J. Artif. Intell. Res.*, vol. 16, no. 1, 2002, Art. no. 321357.

[52] N. Japkowicz, "The class imbalance problem: Signicance and strategies," in *Proc. Int. Conf. Artif. Intell.*, 2000, p. 17.

[53] L. Nanni, C. Fantozzi, and N. Lazzarani, "Coupling different methods for overcoming the class imbalance problem," *Neurocomputing*, vol. 158, p. 4861, Jun. 2015.

[54] L. Demidova and I. Klyueva, "SVM classication: Optimization with the SMOTE algorithm for the class imbalance problem," in *Proc. 6th Medit. Conf. Embedded Comput. (MECO)*, Jun. 2017, p. 14.

[55] W. Mao, L. He, Y. Yan, and J. Wang, "Online sequential prediction of bearings imbalanced fault diagnosis by extreme learning machine," *Mech. Syst. Signal Process.*, vol. 83, Jan. 2017, Art. no. 450473.

[56] *The GAN Zoo: A List of All Named GANs*. Accessed: Jun. 14, 2019. [Online]. Available: https://github.com/hindupuravinash/the-gan-zoo

[57] S. K. Lim, Y. Loo, N.-T. Tran, N.-M. Cheung, G. Roig, and Y. Elovici, "DOPING: Generative data augmentation for unsupervised anomaly detection with GAN," in *Proc. IEEE Int. Conf. Data Mining (ICDM)*, Nov. 2018, Art. no. 11221127.

[58] A. Radford, L. Metz, and S. Chintala, "Unsupervised representation learning with deep convolutional generative adversarial networks," 2015, *arXiv:1511.06434*. [Online]. Available: http://arxiv.org/abs/1511.06434

[59] P. Isola, J.-Y. Zhu, T. Zhou, and A. A. Efros, "Image-to-Image translation with conditional adversarial networks," in *Proc. IEEE Conf. Comput. Vis. Pattern Recognit. (CVPR)*, Jul. 2017, pp. 5967–5976, doi: 10.1109/CVPR.2017.632.

[60] T. Salimans, I. Z. W. Goodfellow, V. Cheung, A. Radford, and X. Chen, "Improved techniques for training GANs," in *Proc. Adv. Neural Inf. Process. Syst.*, 2016, pp. 2234–2242.

[61] V. Sampath, I. Maurtua, J. J. Aguilar Martín, and A. Gutierrez, "A survey on generative adversarial networks for imbalance problems in computer vision tasks," *J. Big Data*, vol. 8, no. 1, p. 27, Dec. 2021, doi: 10.1186/s40537-021-00414-0.

[62] J. Lee and K. Park, "GAN-based imbalanced data intrusion detection system," *Pers. Ubiquitous Comput.*, vol. 25, no. 1, pp. 121–128, Feb. 2021, doi: 10.1007/s00779-019-01332-y.

[63] J. Engelmann and S. Lessmann, "Conditional wasserstein GAN-based oversampling of tabular data for imbalanced learning," *Expert Syst. Appl.*, vol. 174, Jul. 2021, Art. no. 114582, doi: 10.1016/j.eswa.2021.114582.

[64] L. Tian, G. Sihai, and L. Hongjie, "Research on fault diagnosis method of aluminum electrolytic cell based on feature extraction," in *Proc. 32nd Youth Academic Annu. Conf. Chin. Assoc. Autom. (YAC)*, May 2017, pp. 127–131, doi: 10.1109/YAC.2017.7967391.

[65] E. Sun, M. Wang, Z. Li, J. Li, and D. Gao, "Diagnosis and decision analysis system of high temperature molten aluminum cell based on neural network," in *Proc. IEEE 4th Inf. Technol., Netw., Electron. Autom. Control Conf. (ITNEC)*, Jun. 2020, pp. 1624–1628, doi: 10.1109/ITNEC48623.2020.9085003.

[66] C. Xiaofang, Y. Xiaowei, and H. Keke, "Identification of superheat of aluminum electrolytic cell based on computer vision and expert rule," in *Proc. Chin. Autom. Congr. (CAC)*, Oct. 2017, pp. 4705–4710, doi: 10.1109/CAC.2017.8243610.

[67] A. P. Mathur and N. O. Tippenhauer, "SWaT: A water treatment testbed for research and training on ICS security," in *Proc. Int. Workshop Cyber-Phys. Syst. Smart Water Netw. (CySWater)*, Apr. 2016, pp. 31–36.

[68] C. M. Ahmed, V. R. Palleti, and A. P. Mathur, "WADI: A water distribution testbed for research in the design of secure cyber physical systems," in *Proc. 3rd Int. Workshop Cyber-Phys. Syst. Smart Water Netw.*, Apr. 2017, pp. 25–28.

DANYANG CAO received the B.S. and M.S. degrees in computer science and technology from the North China University of Technology, China, in 2000 and 2006, respectively, and the Ph.D. degree in computer application technology from the University of Science Technology Beijing, China, in 2012. He is currently a Professor with the School of Information Science and Technology, North China University of Technology. He also works with the Beijing Key Laboratory on Integration and Analysis of Large-Scale Stream Data. His research interests include artificial intelligence and data mining.

DI LIU received the B.S. degree from the School of Computer, North China Institute of Science and Technology, in 2019. He is currently pursuing the degree with the North China University of Technology.

XU REN received the B.S. degree from the School of Computer, Beijing University of Civil Engineering and Architecture, in 2018. He is currently pursuing the degree with the North China University of Technology.

NAN MA (Senior Member, IEEE) received the Ph.D. degree in computer application technology from the University of Science Technology Beijing, China, in 2012. She is currently a Professor with the College of Robotics, Beijing Union University, China. Her research interests include artificial intelligence and data mining.

• • •